THE JOURNAL OF BIOLOGICAL CHEMISTRY
Vol. 276, No. 52, Issue of December 28, pp. 48637–48643, 2001
Printed in U.S.A.

Phosphoisoprenoids Modulate Association of Rab Geranylgeranyltransferase with REP-1*

Received for publication, August 27, 2001, and in revised form, October 4, 2001
Published, JBC Papers in Press, October 23, 2001, DOI 10.1074/jbc.M108241200

Nicolas H. Thomä‡, Andrei Iakovenko, Roger S. Goody, and Kirill Alexandrov§

From the Department of Physical Biochemistry, Max-Planck-Institute for Molecular Physiology, Otto-Hahn-Strasse 11, 44227 Dortmund, Germany

Rab geranylgeranyltransferase (RabGGTase or GGTase-II) catalyzes the post-translational prenylation of Rab proteins. Rab proteins are recognized as substrates only when they are complexed to Rab Escort Protein (REP). The classical model of prenylation complex assembly assumes initial formation of the Rab·REP binary complex, which subsequently binds to RabGGTase loaded with the isoprenoid donor geranylgeranyl pyrophosphate (GGpp). We demonstrate here that REP-1 can also associate with RabGGTase in the absence of Rab protein and that this interaction is dramatically strengthened by the presence of phosphoisoprenoids such as GGpp. The GGpp-dependent interaction between RabGGTase and REP-1 was observed using affinity precipitations and gel filtration and was quantitated on the basis of fluorescence assays. In the presence of GGpp, REP-1 binds to RabGGTase with a K_d value of ~10 nM, while in its absence the affinity between the two proteins is in the micromolar range. We further demonstrate that binding of Rab7 to the RabGGTase·GGpp·REP-1 complex occurs without prior dissociation of REP-1. Analysis of binding and prenylation rate constants indicate that the RabGGTase·GGpp·REP-1 complex can function as a kinetically competent intermediate of the prenylation reaction. We conclude that, depending on the prevailing concentrations, binding of REP-1 to RabGGTase in the presence of GGpp may serve as an alternative pathway for the assembly of the prenylation machinery *in vivo*. Implications of these findings for the role of REP-1 in the prenylation reaction are discussed.

Rab proteins are members of the Ras superfamily of small GTP-binding proteins, which are directly implicated in the regulation of vesicular traffic (1). They are rendered functionally active by post-translational lipidation, which is conferred by Rab geranylgeranyltransferase (RabGGTase or GGTase-II). This enzyme attaches two hydrophobic geranylgeranyl moieties onto the C-terminal cysteine residues of Rab proteins, thereby enabling them to associate reversibly with membranes. Mammalian RabGGTase is a heterodimer composed of tightly associated α and β subunits and belongs to the family of protein prenyltransferases together with geranylgeranyltransferase I and farnesyltransferase (2). The crystal structure of RabGGTase revealed that the phosphoisoprenoid binding site is located in a buried cavity on the β subunit (3). The α subunit consists of a helical domain, followed by an immunoglobulin (Ig)-like fold and an additional leucine rich repeat. In contrast to other known prenyltransferases, RabGGTase binds its protein substrate sufficiently tightly only if it is complexed to an accessory factor, termed Rab Escort Protein (REP)[1] (2, 4). In the absence of REP the affinity of Rab proteins toward RabGGTase was estimated to be in the micromolar range (5). It has been shown that RabGGTase can bind a variety of Rab proteins with comparable affinities (6, 7). Moreover, it was suggested that RabGGTase binds the REP·Rab complex primarily through the interaction with REP, and both the leucine rich repeat and Ig domains of RabGGTase were implicated in the recognition process (3, 7, 8).

According to the current model, a newly synthesized Rab protein forms a stable complex with REP. The resulting binary complex is then recognized by RabGGTase, which covalently attaches a geranylgeranyl moiety to the C-terminal cysteines of the Rab protein (9). Upon prenylation, Rab remains bound to REP and accompanies it to the corresponding membrane (10, 11). The Rab protein is inserted into the membrane, presumably through the interaction with a putative membrane receptor/REP-GDP dissociation inhibitor displacing factor (10, 12, 13). Subsequently, REP is released into the cytosol and can enter a new prenylation cycle.

We demonstrate here that RabGGTase is able to bind directly to REP-1 in the presence of phosphoisoprenoids. The affinity for formation of this complex is in the low nanomolar range, while micromolar affinities are observed in the absence of GGpp. Furthermore, we show that the RabGGTase·GGpp·REP-1 complex constitutes a kinetically competent intermediate in the prenylation reaction.

EXPERIMENTAL PROCEDURES

Protein Expression, Purification, and Modification—Expression of rat RabGGTase and REP-1 in SF21 cells and subsequent purification was performed as described (14, 15). Construction of dansyl-labeled Rab7 was performed as described (5). The GDP-bound form of Rab7C205SC207S mutant was generated as described (15). *In vitro* prenylation and purification of doubly prenylated dansylated Rab7·REP-1 complex was performed as described (16). Loading of Rab7 with mantGDP was performed as described (17).

Analytical Gel Filtration Chromatography—Protein complex formation was performed in 500 μl of 40 mM Hepes, pH7.2, 150 mM NaCL, 5 mM DTE, 3 mM $MgCL_2$, 90 μM GGpp. The sample was mixed, centrifuged in a bench top centrifuge for 5 min, loaded onto a Superdex 200 10/20 gel filtration column driven by a Waters 490E HPLC system, and equilibrated with 40 mM Hepes, pH7.2, 150 mM NaCL, 5 mM DTE, 3 mM

* This work was supported in part by Deutsche Forschungs-Gemeinschaft Grant AL 484/5-1 (to K. A.). The costs of publication of this article were defrayed in part by the payment of page charges. This article must therefore be hereby marked "*advertisement*" in accordance with 18 U.S.C. Section 1734 solely to indicate this fact.

‡ Supported by the European Molecular Biology Organization long term fellowship. Present address: Memorial Sloan Kettering Cancer Center, Howard Hughes Medical Institute, 1275 New York Ave., New York, NY 10021.

§ To whom correspondence should be addressed. Tel.: 49-231-133-2356; Fax: 49-231-133-1651; E-mail: kirill.alexandrov@mpi-dortmund.mpg.de.

[1] The abbreviations used are: REP, Rab escort protein; DTE, dithioerythritol; HPLC, high pressure liquid chromatography.

$MgCL_2$, 2.3 μM GGpp. The column was calibrated using a gel filtration calibration kit (Bio-Rad). Flow rate was 0.7 ml/min. Peaks were collected and analyzed by SDS-PAGE followed by Coomassie Blue staining.

Steady-state Fluorescence Measurements—Fluorescence titrations were performed with an Aminco SLM 8100 spectrophotometer (Aminco, Silver Spring, MD). All reactions were followed at 25 °C in 25 mM Hepes, pH 7.2, 40 mM NaCl, 100 mM NaH_2PO_4, 2 mM $MgCl_2$ and 2 mM DTE in 1 ml volume, unless otherwise indicated. The fluorescence of mant-farnesyl pyrophosphate (mFpp) was excited via FRET at 290 nm, and emission was measured at 335 nm.

Analysis of Fluorescence Titrations—Titrations were fitted to the explicit solution of the quadratic equation describing the $E + S <> ES$ binding equilibrium, where K_d is defined as $K_d = [E]*[S]/[EL]$. $[E_0]$ and $[L_0]$ refer to the total enzyme and ligand concentration (free and bound) in the cuvette. Under these conditions the fluorescence is described by

$$F = F_{min} + (F_{max} - F_{min})/\cdot (([E_0] + [L_0] + K_d)/2 - ([E_0] + [L_0] + K_d)^2/4 - [E_0]*[L_0])^{1/2}/[L_0] \quad \text{(Eq. 1)}$$

where F represents the measured fluorescence intensity, and F_{min} and F_{max} refer to the minimal and maximal fluorescence intensity observed, respectively. A least-squares fit of the data to Equation 1 using the software package Grafit 4.0 (Erithacus software) was used to extract the K_d value.

Transient Kinetics Experiments—Stopped flow experiments were performed in a High-Tech Scientific SF61 apparatus (Salisbury, England). The tryptophan fluorescence was excited at 290 and detected through a 333-nm cutoff filter. Data collection and primary analysis of rate constants were performed with the package from High Tech Scientific, and secondary analyses were performed with the programs Grafit 3.0 (Erithacus software) and Scientist 2.0 (MicroMath Scientific Software). Traces showed a contribution from photo-bleaching and were fitted as single exponential function with a slope $(A*\exp(-k*t)+m*t)$, where A is the observed amplitude, k the observed rate constant for the reaction, and m the essentially linear slope of the beginning of the bleaching curve.

Immobilization of RabGGTase on Sepharose Beads—RabGGTase was coupled to UltraLink™ (Pierce) beads via a reactive cysteine linkage according to the instructions of the manufacture. Approximately 2 mg of protein was coupled per ml of drained beads.

Pull-down Assays—Ni-NTA-agarose beads (Qiagen) were pre-equilibrated with incubation buffer containing 40 mM Hepes, pH 7.2, 150 mM NaCl, 1 mM $MgCl_2$, 0.005% Triton X-100, and 2 mM β-mercaptoethanol and saturated with REP-1. For precipitation experiments, ~30 μl of drained beads were mixed with 20 pmol of REP-1 and RabGGTase. The total reaction volume was brought to 500 μl with incubation buffer, and GGpp was added to 2 μM where appropriate. After 10 min of incubation, beads were pelleted by centrifugation in a bench top centrifuge at 3000 × *g* for 3 min and washed five times with the reaction buffer supplemented with GGpp where required. Bound material was eluted by boiling beads in 50 μl of loading buffer and analyzed by SDS-PAGE followed by Coomassie blue staining. Identical conditions were used for precipitation of REP-1 with RabGGTase immobilized on Sepharose beads.

In Vitro Prenylation Assay—Development of the HPLC assay for analysis of the kinetics of the prenylation reaction will be described in detail elsewhere[2] but is outlined briefly here. The reactions were performed in glass tubes using the following reaction buffer: 40 mM Hepes, pH 7.2, 150 mM NaCl, 5 mM DTE, 3 mM $MgCl_2$, and 0.3% Nonidet P-40. For kinetic measurements, 4 μM Rab7 and 4 μM REP-1·RabGGTase complex were pre-incubated separately in the presence of 40 μM GGpp for 5 min at 25 °C. The reaction was initiated by manual mixing of Rab7 and REP-1·RabGGTase. After defined time periods, 50 μl of the reaction mixture was withdrawn, quenched by addition of 100 μl of 0.3% trifluoroacetic acid,20% glycerol mix, and flash frozen in liquid nitrogen. For analysis, 75 μl of quenched reaction mix was subjected to reverse phase chromatography. Samples were analyzed using a C4, 150 × 4.6-mm, 15 μm LUNA column (Phenomenx) driven by a Waters 600 s HPLC. The column was equilibrated with 95% buffer A (0.1% trifluoroacetic acid in water) and 5% buffer B (0.1% trifluoroacetic acid in acetonitrile) at a flow rate of 1 ml/min. After injection and a 2-min wash step, proteins were eluted with a gradient from 5–70% of buffer B in 15 min. A Waters 2487 diode-array absorbance detector was used to simultaneously monitor absorbance at 210 nm and 280 nm. The primary HPLC data analysis was performed by integrating peak areas using the Waters Millennium software package. Data was analyzed by numerical integration to the explicit reaction scheme described in Thomä and Alexandrov.[2]

RESULTS

We have previously established that RabGGTase binds the Rab7·REP-1 complex with a K_d close to 100 nM (15). It was assumed that the presence of Rab is required for the tight interaction between RabGGTase and REP-1. Careful analysis of solid phase precipitation assays revealed, however, that trace amounts of RabGGTase co-precipitate with REP-1 in the absence of Rab7 protein (Fig. 1 in Ref. 15). This could in principle indicate that RabGGTase is able to bind REP-1 directly, albeit with low affinity. Moreover, based on similar affinities for REP observed for different Rab proteins, it had been suggested that the interaction between RabGGTase and Rab·REP is dominated by REP rather than Rab (7). Finally, we demonstrated earlier that GGpp dramatically increases the affinity of RabGGTase for the Rab·REP complex (16). These observations prompted us to re-examine the issue of direct association of REP with RabGGTase and to address the role of phosphoisoprenoids in this interaction.

RabGGTase and REP-1 Co-precipitate in the Presence of GGpp—To detect the interaction of RabGGTase and REP-1, we performed solid state precipitation assays. To this end, RabGGTase was immobilized on Sepharose beads and REP-1 was immobilized on Ni-NTA-agarose as described under "Experimental Procedures." The beads were incubated with solutions of REP-1 and RabGGTase, respectively, in the presence or absence of 2 μM GGpp. The beads were subsequently extensively washed and pelleted by centrifugation. The washing step included 2 μM GGpp where previous incubations had been carried out in the presence of phosphoisoprenoid. The bead associated proteins were eluted and resolved on a 15% SDS-PAGE followed by Coomassie stain. As can be seen in Fig. 1, REP-1 co-precipitated with RabGGTase in the presence of GGpp. Co-precipitation appeared to be nearly stoichiometric, suggesting tight interaction of RabGGTase and REP-1 in the presence of GGpp. However, in the absence of lipid substrate, REP-1 did not co-precipitate with bead-linked RabGGTase (Fig. 1). In the reverse experiment, only trace amounts of RabGGTase were found to co-precipitate with bead-bound REP-1 in the absence of GGpp while robust co-precipitation was observed in its presence (Fig. 1). These observations suggest that the presence of GGpp strongly increases the affinity of an otherwise weak binary complex.

Stoichiometry of RabGGTase·GGpp·REP-1 Complex—To determine the stoichiometry of the binary complex we employed analytical gel filtration on a Superdex 200 column. When REP-1 was mixed with an excess of RabGGTase and GGpp, two peaks of about 210 kDa and 100 kDa were recovered (Fig. 2*A*). As revealed by SDS-PAGE, the 210-kDa peak contained REP-1 and RabGGTase in a 1:1 ratio as judged from the intensity of the Coomassie stained bands (Fig. 2*B*). Judging from the composition and the retention time this peak contains the ternary RabGGTase·GGpp·REP-1complex. The smaller peak contained predominantly subunits of RabGGTase with a minor contamination of REP-1. In this case both proteins elute at their monomeric positions. Since samples of REP-1 are known to be contaminated with unspecific phophatase activity, we speculated that it might lead to degradation of GGpp and dissociation of the complex (15, 18). Indeed, when the same experiment was repeated using a non-hydrolyzable phosphoisoprenoing analog instead of GGpp, no REP-1 contamination was observed in the 90-kDa peak.[3]

[2] Thomä, N. H., Niculae, A., Goody, R. S., and Alexandrov, K. (2001) *J. Biol. Chem.* **276,** 48631–48636.

[3] A. Rak and K. Alexandrov, submitted for publication.

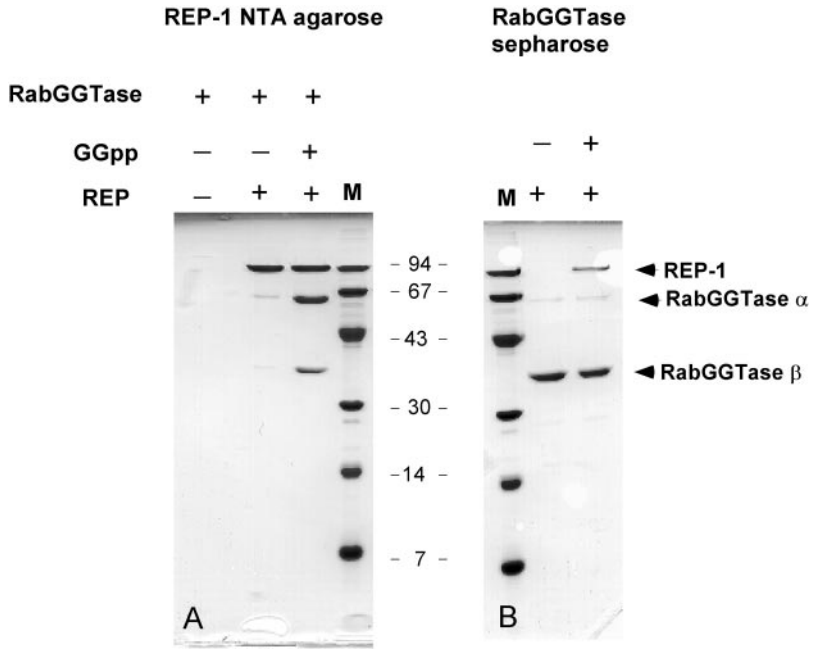

FIG. 1. **Detection of RabGGTase·GGpp·REP-1 complex by affinity precipitations.** Precipitation experiments were carried out with REP-1 bound to Ni-NTA-agarose (*A*) or RabGGTase linked to Sepharose beads (*B*). After incubation, the samples were washed with the incubation buffer, aliquots of the pellet were analyzed by 15% SDS-PAGE, and the proteins were visualized by Coomassie Blue staining. In *A*, effective co-precipitation of RabGGTase with REP-1 beads was observed only in the presence of GGpp. In its absence only trace amounts of RabGGTase precipitated with REP-1. *B*, RabGGTase precipitated REP-1 only in the presence of GGpp. Upon elution α subunit remains associated to the beads. *Horizontal arrows* denote the position of migration of REP-1 and α and β subunits of RabGGTase.

Affinity of RabGGTase·REP-1 Complex in the Presence of Phosphoisoprenoid—The interaction of RabGGTase and REP-1 was monitored and quantitated by fluorescence titrations in the presence of a fluorescent analog of GGpp (mFpp) (18, 19). First, we titrated 200 nM of the RabGGTase·mFpp complex with increasing concentrations of REP-1. Under the experimental conditions used, essentially all of the isoprenoid is complexed with the enzyme due to the high affinity of this interaction (~30 nM) (18). There was a saturable increase in direct fluorescence intensity following the addition of REP-1 (Fig. 3). Analysis of the stoichiometry indicated that one mole of REP-1 bound to one mole of the RabGGTase·mFpp complex (Fig. 3). A least-squares fit of the data to a quadratic equation led to a K_d value of 10 ± 2 nM.

Kinetics of REP-1 Interaction with RabGGTase·GGpp Complex—The kinetics of REP-1 binding to the RabGGTase·GGpp complex were studied by rapid mixing methodology utilizing changes in the tryptophan fluorescence upon REP-1 binding to the RabGGTase·GGpp complex. In a typical experiment, 100 nM RabGGTase was mixed with different concentrations of REP-1 in the presence of 2 μM GGpp. Fluorescence decreased on mixing RabGGTase and REP-1 in the presence of GGpp (Fig. 4) but not in its absence (data not shown). A similar decrease was observed in the presence of farnesyl pyrophosphate but not of geranyl pyrophosphate (data not shown). The secondary plot of the observed rate constants (k_{obs}) against the concentration of REP-1 is shown in Fig. 4*B*. A linear fit of the data yielded a second order rate constant of 0.08 nM^{-1} s^{-1} (Fig. 4*B*). The dissociation rate constant (k_{off}), inferred form of the intercept of the linear fit with the ordinate, was not well defined (Fig. 4*B*). When the reaction mixture was supplemented with Fpp instead of GGpp, the inferred k_{off} was distinctly larger, indicating weaker binding (Fig. 4*C*). To measure the dissociation rate of the RabGGTase·GGpp·REP-1 directly, 100 nM RabGGTase and 100 nM REP-1 were mixed with a large molar excess (700 nM) of double prenylated dansyl-labeled Rab7·REP-1 complex (*dans*Rab7GG·REP-1) in the presence of 1 μM GGpp (16). The prenylated *dans*Rab7·REP-1 complex can only associate with the transferase once the latter dissociates from the RabGGTase·GGpp·REP-1 complex. At high concentrations of the *dans*Rab7GG·REP-1 complex, the observed rate reflects the dissociation rate of RabGGTase from REP-1·GGpp complex. The obtained transient is shown in Fig. 4*D*. Fitting the data to a single exponential function resulted in k_{obs} = 0.5 s^{-1}. A further increase in the concentration of the *dans*Rab7GG·REP-1 complex did not influence the observed rate constants so that this value represents the genuine k_{off} of RabGGTase from the RabGGTase·GGpp·REP-1 complex. On the basis of dissociation and association rate constants, the affinity of REP-1 to the RabGGTase·GGpp complex was calculated as K_d = 0.5 s^{-1}/0.08 nM^{-1} s^{-1} = 6.25 nM, which is in a good agreement with the equilibrium measurements.

It remains unclear up to this point whether the RabGGTase·GGpp·REP-1 ternary complex is a catalytically competent intermediate *en route* to double prenylation. We therefore set out to determine the binding and prenylation rate constants of different prenylation reaction intermediates including the RabGGTase·GGpp·REP-1 complex.

Interaction of Rab7 with the RabGGTase·GGpp·REP-1 Complex—If binding of REP-1 to the RabGGTase·GGpp complex is the first step in the prenylation machinery assembly, then association of Rab7 with ternary complex must occur in the next step. We measured the association rate constant of Rab7 to the ternary complex. To study binding independently of catalysis, we chose a mutant Rab7(C205SC207S), in which all prenylatable cysteine residues are replaced by serine (Rab7SS). This mutant was previously shown to interact with REP-1 and RabGGTase with kinetics similar to those of wild type protein (15, 16). For determination of the association kinetics, 100 nM of Rab7SS loaded with mantGDP was rapidly mixed with increasing concentrations of the RabGGTase·REP-1 complex in the presence of 2 μM GGpp. Under the chosen conditions, the RabGGTase·GGpp·REP-1 complex can be viewed as a single entity, since the chosen concentrations of components are far above the K_d for their interaction. The observed single exponential rate constants were plotted against the concentration of the RabGGTase·GGpp·REP-1 complex. Fitting the data resulted in an association rate constant (k_{on}) of 0.0012 nM^{-1} s^{-1} for Rab7 binding to the RabGGTase·GGpp·REP-1 complex (Fig. 5*A*).

Next, we measured the dissociation rate constant of Rab7 from the RabGGTase·GGpp·REP-1·Rab7 complex. 250 nM mantGDP·Rab7SS, 250 nM REP-1 and 2 μM RabGGTase were mixed rapidly with 2 μM Rab7SS in the presence of 2 μM GGpp.

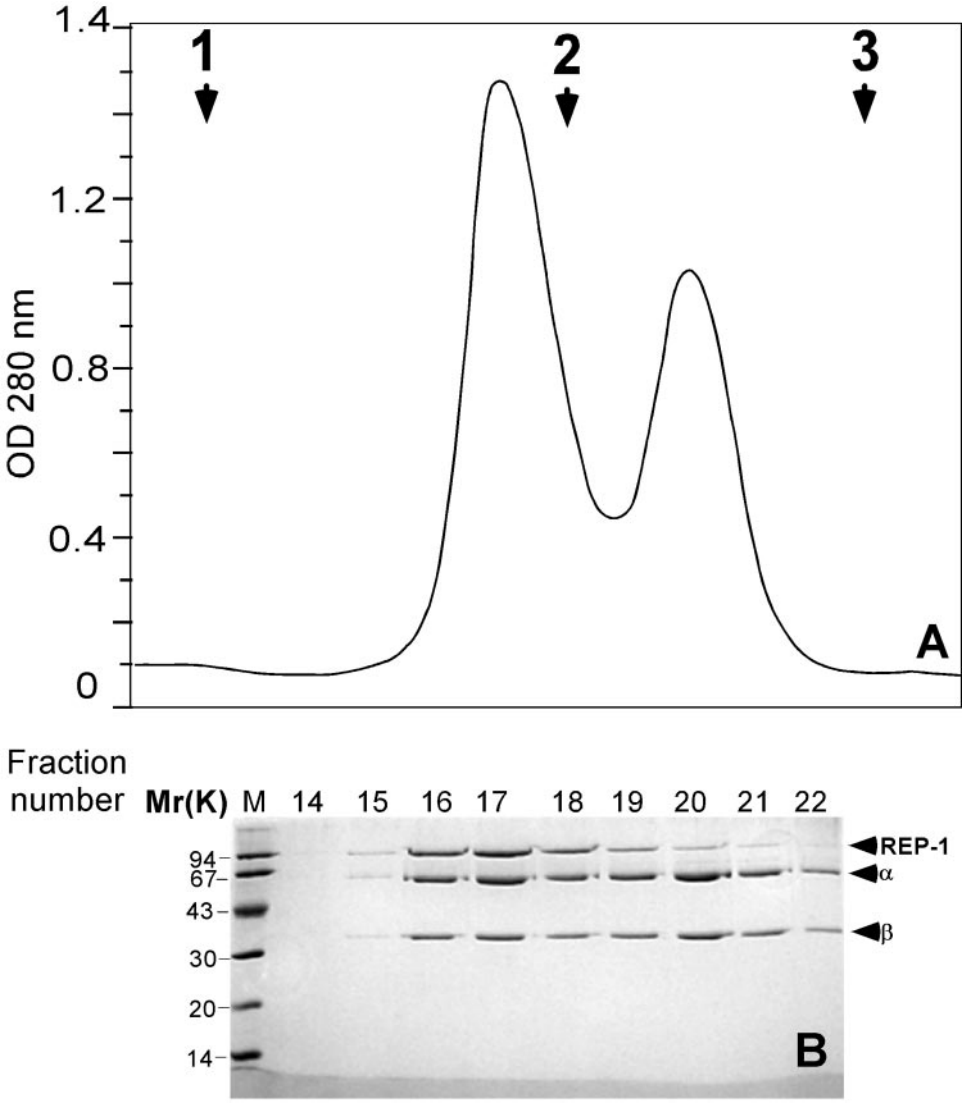

FIG. 2. **Detection of the RabGGTase·GGpp·REP-1 complex by gel filtration chromatography.** The reaction mixture contained 6 μM REP-1, 12 μM RabGGTase, and 46 μM GGpp. After short incubation and centrifugation the sample was loaded onto a Superdex 200 10/20 column equilibrated and run with the flow rate of 0.7 ml/min as described under "Experimental Procedures." Molecular mass of peaks were determined by comparison with protein standards of known molecular mass (1–670 kDa, 2–158 kDa, and 3–44 kDa that are shown as *arrow heads* on *A*. The peaks were subjected to SDS gel electrophoresis on 15% mini-gels, and the proteins were visualized by Coomassie Blue staining (*B*). *Horizontal arrows* denote the position of migration of REP, α and β subunits of RabGGTase, and the molecular mass markers (*left side*).

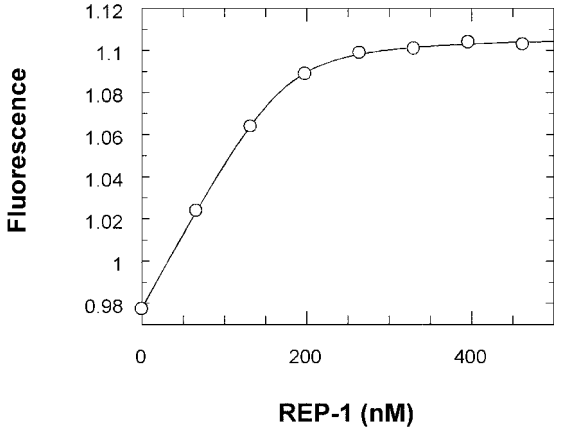

FIG. 3. **Determination of the affinity of REP-1 toward the RabGGTase·mFpp complex.** 200 nM of RabGGTase·mFpp complex were titrated with increasing concentrations of REP-1. By inspection and from the fitting procedure, a 1:1 stoichiometry of the interaction was deduced. The signal was a direct fluorescence of mFpp exciting at 356 nm and monitoring emission at 435 nm.

The observed decrease in fluorescence is due to dissociation of the labeled mGDP·Rab7SS from the complex, followed by association of the excess unlabeled Rab7SS. We determined the dissociation rate constant to be 0.0337 s^{-1}. Based on the ratio of association and dissociation rate constants, the affinity of Rab7 to the RabGGTase·REP-1·GGpp complex could be calculated as K_d = 0.037 s^{-1}/0.0012 nM^{-1} s^{-1} = 28 nM.

To determine which of the two possible routes is taken in the assembly of the prenylation machinery, it is necessary to identify the rate-determining steps. The currently available kinetic and equilibrium constants of the prenylation reaction are summarized in Scheme 1. At high concentrations of RabGGTase, REP-1, Rab7, and GGpp, the second prenylation event, converting singly to doubly prenylated Rab7 is mostly rate-determining (6, 15, 16).[2] At low concentrations of components, when the dissociation rates govern the kinetics, binding of Rab7 to REP-1 and the second prenylation step would become rate-limiting (Scheme 1). To assess the feasibility of RabGGTase·GGpp·REP-1 as a reaction intermediate, we determined the rate of prenylation upon exposure of Rab7 to this complex.

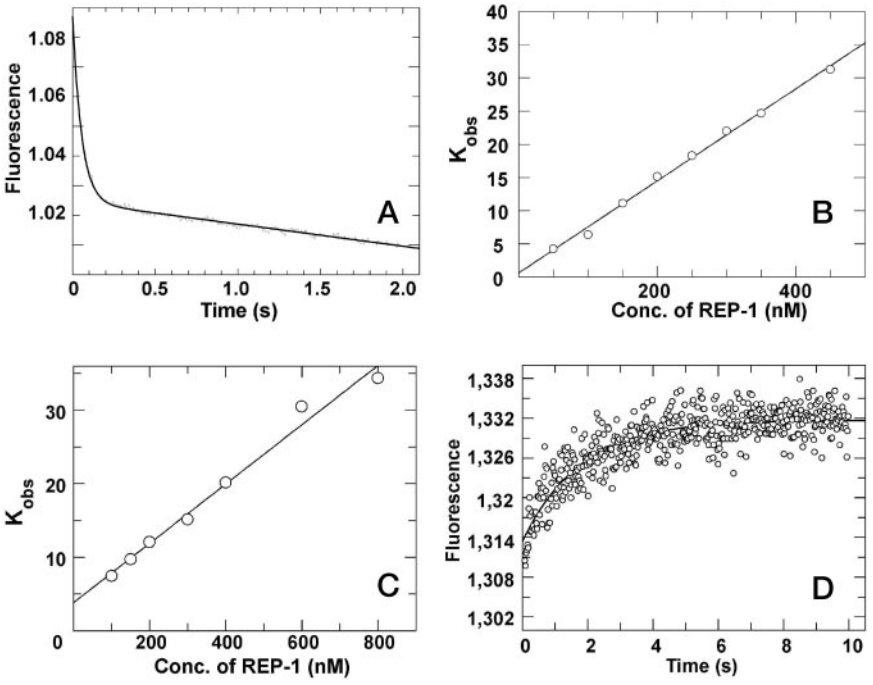

FIG. 4. **Transient kinetic experiments examining binding of REP-1 to RabGGTase in the presence of excess GGpp.** *A*, a typical stopped-flow trace resulting from mixing of 100 nM RabGGTase with 500 nM REP-1 in the presence of 2 μM GGpp. The tryptophan fluorescence was excited at 290 nm, and emission was followed through a 320-nm cut-off filter. The observed stopped-flow transients were fitted using a single exponential function with a slope allowing for the observed photo-bleaching. *B*, plot of the observed rate constants *versus* concentration of REP-1. *C*, plot of the observed rate constants *versus* concentration of REP-1 when the reaction was performed with 2 μM of Fpp instead of GGpp. *D*, fluorescent signal change upon mixing RabGGTase·GGpp·REP-1 complex with excess of prenylated *dans*Rab7·REP-1 complex. The signal used was the change in FRET signal exciting at 288 nm and detecting emission through a 389-nm cut-off filter.

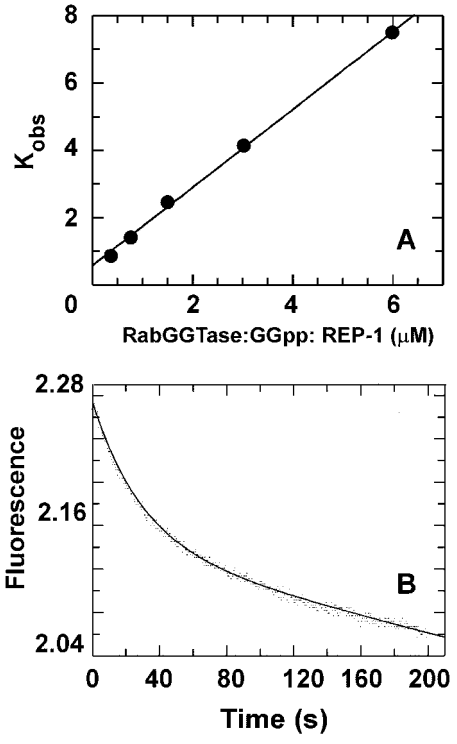

FIG. 5. *A*, secondary plot of observed rate constants obtained by mixing mantGDP·Rab7·(0.2 μM) with increasing concentrations of RabGGTase·GGpp·REP-1 complex in the stopped flow machine. Excitation was at 289 nm, and emission was detected through a 320-nm cut-off filter. *B*, time course of the energy transfer signal change seen on mixing RabGGTase (0.2 μM) and mantGDP·Rab7SS·REP-1 (0.25 μM) with GDP·Rab7SS (2 μM) in the presence of 2 μM of GGpp in the stopped flow machine. Excitation was at 289 nm, and emission was detected through a 320-nm cut-off filter. The fit shown is to a single exponential with slope correcting for the photo-bleaching with a rate constant k_1 for the displacement of mantGDP·Rab7SS with GDP·Rab7SS of 0.0337 s^{-1}.

Rate Constants of REP-1·RabGGTase·GGpp Mediated Prenylation of Rab7—We used an *in vitro* prenylation based on changes in the retention time of Rab7 on the reversed phase matrix upon prenylation.[2] The main advantage of this assay is that it allows parallel monitoring of the rates of single and double prenylation. Rab7 was mixed with a preformed RabGGTase·GGpp·REP-1 complex in the presence of excess GGpp. Aliquots of the reaction mixture were removed at defined time points and analyzed. The observed transients for the decay of Rab7 and the production of double prenylated Rab7 (Rab7_GG) are shown in Fig. 6. Formation of singly prenylated Rab7 proceeded with $k_1 = 0.20 \pm 0.04$ s^{-1}, while the rate constant for conversion of singly into double prenylated Rab7 was $k_2 = 0.029 \pm 0.007$ s^{-1}. These are close to the rate constants determined for mixing the Rab7·REP-1 complex with RabGGTase·GGpp complex ($k_1 = 0.16$ s^{-1} and 0.039 s^{-1}).[2] Under the conditions used (4 μM RabGGTase·GGpp·REP-1 complex mixed with 4 μM Rab7), we can use the second order rate constant for the association reaction determined as described above to calculate half-life for the association reaction. This is calculated to be ~0.2 s^{-1}, whereas the half-life for the dissociation of the RabGGTase·GGpp·REP-1 complex into RabGGTase·GGpp and REP-1 is 1.3 s. Thus association to the ternary complex will occur under these conditions. If this were not an active complex in the sense of prenylation ability, it would then have to redissociate at 0.037 s^{-1} before further dissociation to give free REP-1, which could associate in the "correct" form with Rab7. The kinetic data on prenylation mediated by the RabGGTase·GGpp·REP-1 complex rule out this pathway, since it would lead to much slower prenylation than using the standard mixing regime (generation of the Rab7·REP-1 complex followed by binding of RabGGTase·GGpp). Therefore, we conclude that the RabGGTase·GGpp·REP-1 complex represents a functionally relevant interaction between two proteins, and thus generation of the ternary protein complex can occur directly from this binary complex by binding of Rab7. Scheme 1 summarizes the rate constants determined for prenylation proceeding via formation of the GGTase·REP-1·GGpp complex.

DISCUSSION

The traditional view of the Rab escort protein is that of a molecular chaperone that binds to the newly synthesized Rab protein and presents it first to the RabGGTase and, following prenylation, accompanies it to the membrane. In this work we

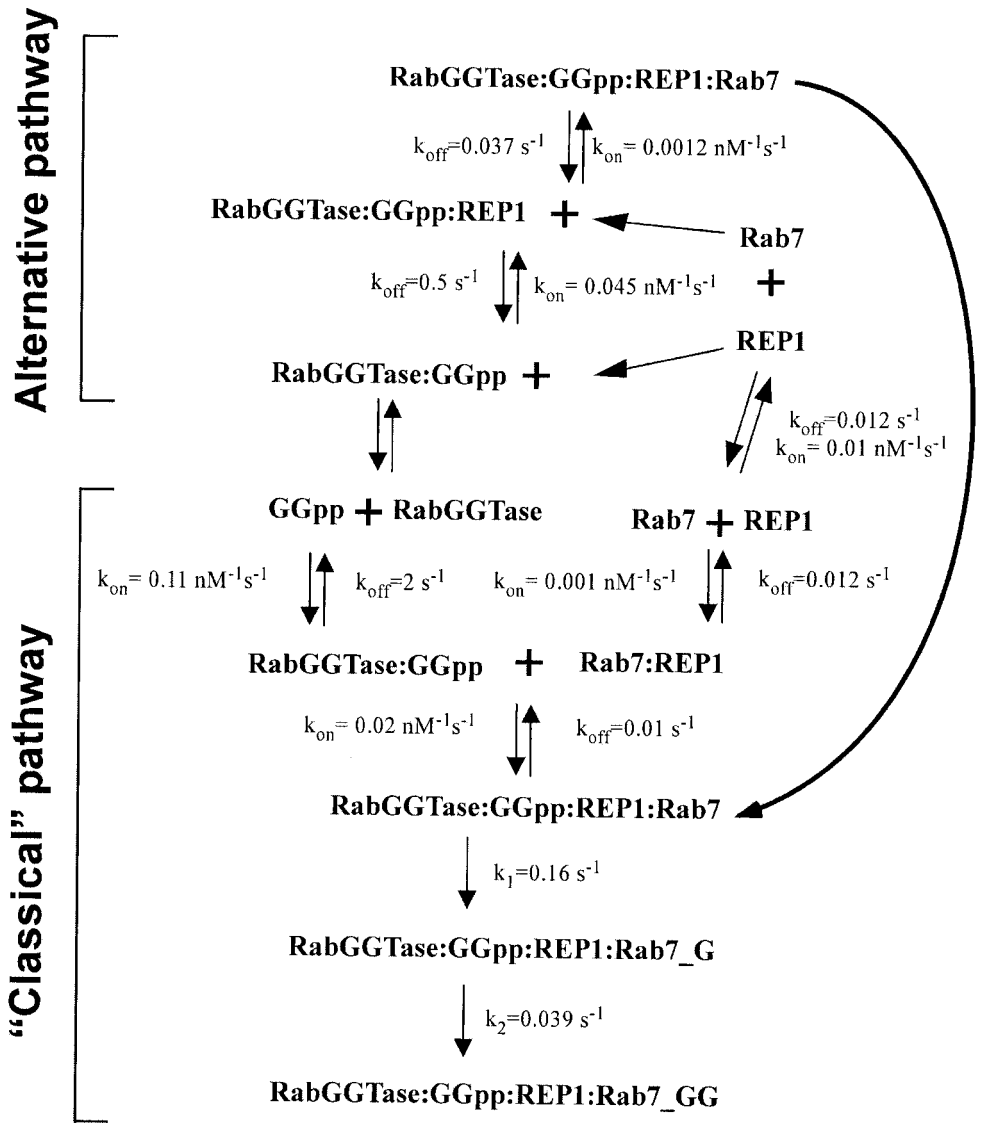

SCHEME 1

have investigated the existence of alternative pathways of the prenylation complex assembly.

Solid phase precipitation assays provided initial evidence that RabGGTase and REP-1 can interact in the presence of GGpp with high affinity. Nearly stoichiometric co-precipitation of REP-1 and the RabGGTase was observed, while essentially no binding could be detected when GGpp was omitted. Fluorescence titrations indicated that REP-1 bound RabGGTase with a 1:1 stoichiometry and an affinity of ~10 nM. Due to the absence of appropriate signals, we could only approximate the binding of RabGGTase to REP in the absence of GGpp as being in the low micromolar range. Significantly, higher affinities can be ruled out based on surface-plasmon resonance experiments[4] and the observed stoichiometry in the solid phase precipitation.

The finding of a tight RabGGTase·GGpp·REP complex contradicts the traditional model of prenylation complex assembly (2, 15, 20) and raises a number of interesting questions. First of all, the role of phosphoisoprenoid in the formation of such complex is quite intriguing, and three models can be considered in this regard. The first possibility is that REP interacts with the active site of RabGGTase via phosphoisoprenoid. However, the observation that the rate of mFpp dissociation from the RabGGTase·mFpp·REP-1 complex is not significantly different from k_{off} of RabGGTase·mFpp complex speaks against this model.[4] The second possibility is that a new phosphoisoprenoid binding site is formed at the interface between RabGGTase and REP with GGpp, thus "gluing" the molecules together. Due to the presence of a canonical lipid binding site on RabGGTase this, however, would result in a 2:1 stoichiometry of phosphoisoprenoid to protein complex. So far, we have found no experimental confirmation of this prediction.[4] Finally, it is conceivable that binding of phosphoisoprenoid induces a conformational change in RabGGTase that leads to complex formation with REP. More experiments will be needed to provide evidence for any of these hypothesis.

It is surprising that such a tight complex has evaded identification for so many years. This is probably attributable to the rapid dissociation rates of the complex. For instance, the RabGGTase·GGpp·REP complex cannot be isolated by gel filtration unless the column is equilibrated in the presence of GGpp (15). If this is not done, phosphoisoprenoid dissociating from the complex is retained by the column much longer than the rapidly migrating proteins.[4]

Finally, we have addressed the question of the kinetic competence of the RabGGTase·GGpp·REP complex. The strategy chosen was to determine the major rate constants governing

[4] K. Alexandrov, unpublished data.

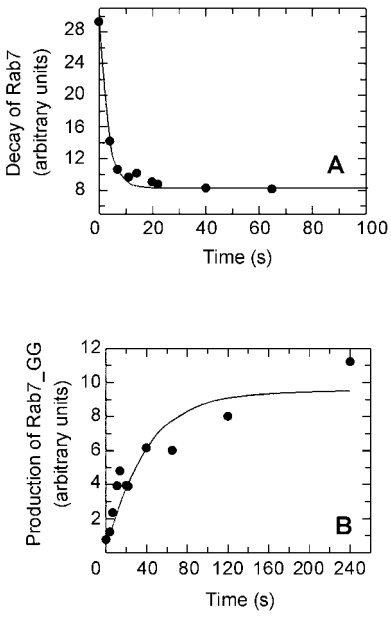

FIG. 6. **Observed time course for mono- and double prenylation of Rab7 mediated by RabGGTase·GGpp·REP-1 complex.** *A*, time course of unprenylated Rab7 decay. The fit shown is to a single exponential equation with a rate constant of k_1 0.28 s^{-1}. *B*, time course of generation of doubly prenylated Rab7. The fit is to a single exponential equation with a rate constant of k_2 0.018 s^{-1}.

the binding of the intermediates that lead to assembly of the quaternary prenylation complex. Rate constants are summarized in Scheme 1. Examination of the association and dissociation rate constants indicate the presence of three time regimes. First, binding of GGpp to the transferase is fast having the highest association and dissociation rate constants. Second, binding of REP-1 to RabGGTase·GGpp is intermediate with dissociation and association being slower than those for GGpp. Finally, binding of Rab7 to the ternary RabGGTase GGpp·REP-1 complex is slow. The measured association rate is 10 times slower than for direct Rab7·REP-1 interaction (6). It is, however, remarkable that both association and dissociation rate constants for all complexes decrease so that the observed affinity at all three steps are comparable and generally lie in the low nanomolar range. Together with the prenylation rate constant, it ensues that the rate-determining step for assembly of the prenylation machinery is dependent on the concentration of all components. At high concentrations of RabGGTase, REP-1, Rab7, and GGpp all binding events are sufficiently fast so that the second prenylation step becomes rate-determining. At low concentrations, however, the kinetics are dominated by the dissociation rate constants of the individual steps. The dissociation rate constant of Rab7 from the RabGGTase·GGpp·REP-1 complex is sufficiently slow that the complex cannot equilibrate before transfer occurs. Additional rate determining steps at low concentration are the prenyl transfer and, also assuming a low concentration of GGpp, product release (16). It follows from this kinetic scheme that under conditions where the concentration of RabGGTase, REP-1 and GGpp are slightly elevated compared with that of Rab the pathway proceeding via the RabGGTase·GGpp·REP-1 intermediate is indeed populated. The RabGGTase·REP-1·GGpp complex can thus constitute a kinetically competent intermediate in the assembly of the prenylation machinery, and the affinities for this interaction are sufficiently tight to be of relevance *in vivo*. The choice between canonical and alternative pathways will depend on the concentration of individual components and may therefore be dependant on the metabolic state of the cell. Currently very little is known about the concentration and localization of phosphoisoprenoids in living cells, and further research will be needed to clarify this point.

What could be the physiological relevance of such a RabGGTase·GGpp·REP-1 complex? One possibility is that the role of REP-1 as a chaperone and transport protein might not be as static as previously believed. Rather than waiting for a Rab protein to be synthesized and then transport it to the membrane, REP-1 could already be in complex with RabGGTase·GGpp. Once Rab is bound, prenylation could quickly be initiated. It should be noted that the rate of double prenylation is surprisingly slow, with a characteristic half-time of more than 30 s. It is conceivable that the entire quaternary complex, composed of RabGGTase·GGpp·REP·Rab, travels toward the membrane while prenylation is occurring. By this mechanism, the two most time-consuming steps in the cycle, namely the prenylation of Rab7 and the transport of the Rab·REP complex to the membrane, could be combined. This is consistent with previous findings that the presence of RabGGTase did not inhibit membrane association of the prenylated Rab5·REP-1 complex (10). Further *in vivo* studies focused on localization of the individual components are required to clarify this issue.

Acknowledgments—Thanks are due to Catherine Katzka for critically reading the manuscript. We acknowledge Stefan Uttich for invaluable technical assistance. Anca Niculae is acknowledged for her help with the gel filtration experiments.

REFERENCES

1. Stenmark, H., and Olkkonen, V. M. (2001) *Genome Biol.* **2,** 1–7
2. Casey, P. J., and Seabra, M. C. (1996) *J. Biol. Chem.* **271,** 5289–5292
3. Zhang, H., Seabra C. M., and Deisenhofer, J. (2000) *Structure* **8,** 241–251
4. Andres, D. A., Seabra, M. C., Brown, M. S., Armstrong, S. A., Smeland, T. E., Cremers, F. P., and Goldstein, J. L. (1993) *Cell* **73,** 1091–1099
5. Iakovenko, A., Rostkova, E., Merzlyak, E., Hillebrand, A. M., Thoma, N. H., Goody, R. S., and Alexandrov, K. (2000) *FEBS Lett.* **468,** 155–158
6. Alexandrov, K., Simon, I., Iakovenko, A., Holz, B., Goody, R. S., and Scheidig, A. J. (1998) *FEBS Lett.* **425,** 460–464
7. Anant, J. S., Desnoyers, L., Machius, M., Demeler, B., Hansen, J. C., Westover, K. D., Deisenhofer, J., and Seabra, M. C. (1998) *Biochemistry* **37,** 12559–12568
8. Alory, C., and Balch, W. E. (2000) *J. Cell Biol.* **150,** 89–103
9. Farnsworth, C. C., Seabra, M. C., Ericsson, L. H., Gelb, M. H., and Glomset, J. A. (1994) *Proc. Natl. Acad. Sci. U. S. A.* **91,** 11963–11967
10. Alexandrov, K., Horiuchi, H., Steele-Mortimer, O., Seabra, M. C., and Zerial, M. (1994) *EMBO J.* **13,** 5262–5273
11. Wilson, A. L., Sheridan, K. M., Erdman, R. A., and Maltese, W. A. (1996) *Bochem. J.* **318,** 1007–1014
12. Dirac-Svejstrup, A. B., Soldati, T., Shapiro, A. D., and Pfeffer, S. R. (1994) *J. Biol. Chem.* **269,** 15427–15430
13. Soldati, T., Shapiro, A. D., and Pfeffer, S. R. (1995) *Methods Enzymol.* **257,** 253–259
14. Armstrong, S. A., Brown, M. S., Goldstein, J. L., and Seabra, M. C. (1995) *Methods Enzymol.* **257,** 30–41
15. Alexandrov, K., Simon, I., Yurchenko, V., Iakovenko, A., Rostkova, E., Scheidig, A. J., and Goody, R. S. (1999) *Eur. J. Biochem.* **265,** 160–170
16. Thoma, N. H., Iakovenko, A., Kalinin, A., Waldmann, H., Goody, R. S., and Alexandrov, K. (2001) *Biochemistry* **40,** 268–274
17. Simon, I., Zerial, M., and Goody, R. S. (1996) *J. Biol. Chem.* **271,** 20470–20478
18. Thoma, N. H., Iakovenko, A., Owen, D., Scheidig, A. S., Waldmann, H., Goody, R. S., and Alexandrov, K. (2000) *Biochemistry* **39,** 12043–12052
19. Owen, D. J., Alexandrov, K., Rostkova, E., Scheidig, A. J., Goody, R. S., and Waldmann, H. (1999) *Angew. Chem. Int. Ed. Engl* **38,** 509–512
20. Pereira-Leal, J. B., Hume, A. N., and Seabra, M. C. (2001) *FEBS Lett.* **498,** 197–200

Phosphoisoprenoids Modulate Association of Rab Geranylgeranyltransferase with REP-1

Nicolas H. Thomä, Andrei Iakovenko, Roger S. Goody and Kirill Alexandrov

J. Biol. Chem. 2001, 276:48637-48643.
doi: 10.1074/jbc.M108241200 originally published online October 23, 2001
